Vol 455|23 October 2008|doi:10.1038/nature07381

nature

LETTERS

# Reassessing the first appearance of eukaryotes and cyanobacteria

Birger Rasmussen[1], Ian R. Fletcher[1], Jochen J. Brocks[2,3] & Matt R. Kilburn[4]

**The evolution of oxygenic photosynthesis had a profound impact on the Earth's surface chemistry, leading to a sharp rise in atmospheric oxygen between 2.45 and 2.32 billion years (Gyr) ago[1,2] and the onset of extreme ice ages[3]. The oldest widely accepted evidence for oxygenic photosynthesis has come from hydrocarbons extracted from ~2.7-Gyr-old shales in the Pilbara Craton, Australia, which contain traces of biomarkers (molecular fossils) indicative of eukaryotes and suggestive of oxygen-producing cyanobacteria[4–7]. The soluble hydrocarbons were interpreted to be indigenous and syngenetic despite metamorphic alteration and extreme enrichment (10–20‰) of $^{13}C$ relative to bulk sedimentary organic matter[5,8]. Here we present micrometre-scale, *in situ* $^{13}C/^{12}C$ measurements of pyrobitumen (thermally altered petroleum) and kerogen from these metamorphosed shales, including samples that originally yielded biomarkers. Our results show that both kerogen and pyrobitumen are strongly depleted in $^{13}C$, indicating that indigenous petroleum is 10–20‰ lighter than the extracted hydrocarbons[5]. These results are inconsistent with an indigenous origin for the biomarkers. Whatever their origin, the biomarkers must have entered the rock after peak metamorphism ~2.2 Gyr ago[9] and thus do not provide evidence for the existence of eukaryotes and cyanobacteria in the Archaean eon. The oldest fossil evidence for eukaryotes and cyanobacteria therefore reverts to 1.78–1.68 Gyr ago and ~2.15 Gyr ago[10,11], respectively. Our results eliminate the evidence for oxygenic photosynthesis ~2.7 Gyr ago and exclude previous biomarker evidence for a long delay (~300 million years) between the appearance of oxygen-producing cyanobacteria and the rise in atmospheric oxygen 2.45–2.32 Gyr ago[1].**

Hydrocarbon biomarkers represent an important source of information about the diversity and evolution of life, but their application to metamorphosed Precambrian rocks has been plagued by contamination from non-indigenous hydrocarbons[5,8,12]. Recent geochemical studies, using rigorous laboratory procedures designed to minimize this problem, recovered traces of hydrocarbon biomarkers[4] from organic-rich shales as old as ~2.7 Gyr[4–7]. The extracted bitumens mainly consisted of *n*-alkanes, methylalkanes and acyclic isoprenoids, but also included complex polycyclic biomarkers such as 2α-methylhopanes and steranes, suggesting the presence of cyanobacteria and eukaryotes, respectively[4–6]. The biomarker results set new minimum ages for fossil evidence of cyanobacteria (previously ~2.15 Gyr old)[11] and eukaryotes (previously between 1.78 Gyr ago and 1.68 Gyr ago)[10]. The presence of biomarkers linked to oxygen-producing cyanobacteria as well as steranes, the biosynthesis of which in extant eukaryotes requires molecular oxygen, also provides the most reliable minimum age for the onset of oxygenic photosynthesis[4–6]. Although the weight of evidence pointed to a probable syngenetic origin for the biomarkers, the possibility of contamination was not entirely ruled out[5]. An ongoing problem for a syngenetic interpretation, acknowledged in previous studies[4–6], is the extreme enrichment in $^{13}C$ of the extracted hydrocarbons relative to the bulk kerogen.

Sedimentary rocks of Neoarchaean age (2.8–2.5 Gyr old) typically contain strongly $^{13}C$-depleted kerogen ($\delta^{13}C_{bulk} < -39‰$)[5,8], which has been interpreted as evidence for the activity of aerobic[13] or anaerobic[14] methanotrophs, possibly fuelled by a methane-rich atmosphere. Hydrocarbons extracted from 2.7–2.6-Gyr-old shales in the Pilbara Craton, Australia, are enriched in $^{13}C$ relative to bulk organic matter by 10‰ to 20‰ ($\delta^{13}C_{n\text{-alkanes}} = -29‰$ to $-26‰$)[5]. This contrasts with patterns in most Phanerozoic source rocks, in which oils tend to be depleted by 1‰ to 3‰ relative to associated kerogens[15], although slightly enriched bitumen has been recorded in some Proterozoic shales[6]. There are two competing hypotheses that attempt to explain the large isotopic discrepancy in the Neoarchaean shales[5,6]. In the first hypothesis the kerogen is interpreted to have consisted of two isotopically distinct components. One fraction was strongly depleted in $^{13}C$ and comprised highly refractory organic debris from methanotrophs ($\delta^{13}C = -80‰$), which yielded only minor volumes of petroleum on maturation. The other fraction was enriched in $^{13}C$ and formed most of the extractable bitumen[6], including lipids from phototrophic organisms ($\delta^{13}C = -26‰$). The alternative hypothesis is that $^{13}C$-enriched bitumens were introduced into the shales by post-Archaean fluids or through anthropogenic contamination[5].

Until recently it had not been possible to distinguish between these two hypotheses. However, the development of ion microprobe techniques for micrometre-scale $^{13}C/^{12}C$ analysis[16] now allows direct measurement of minute residues of solidified oil (pyrobitumen) and kerogen preserved in the matrix of the Neoarchaean shales[17], including samples that originally yielded molecular fossils. Specifically, *in situ* carbon isotopic analysis of the kerogen and pyrobitumen can test whether oil generated by means of thermal maturation was enriched in $^{13}C$ by 10–20‰ relative to kerogen, as suggested from the isotopic composition of the solvent-extracted hydrocarbons[4–6].

In this study we have examined organic-rich shale from the ~2.63-Gyr-old Roy Hill Shale Member of the Jeerinah Formation, Fortescue Group, from three diamond-drill holes (WRL-1, DDH 186 and FVG-1) in the southern Pilbara Craton, Australia. In this region, mineral assemblages in basalts from the Fortescue Group suggest that the shales have undergone prehnite–pumpellyite facies metamorphism (200–300 °C)[18], consistent with kerogen hydrogen:carbon ratios of 0.1 to 0.3 (refs 5, 8). Heating at these temperatures is estimated to produce a ~1–3‰ enrichment of $^{13}C$ in the organic matter owing to preferential release of $^{13}C$-depleted mobile hydrocarbons during progressive maturation[19].

Petrographic examination shows that most samples contain micrometre-sized residues of organic carbon dispersed in the shale matrix. The organic carbon may occur as bands (>0.1-mm thick) of near-continuous, anastomosed laminae (Fig. 1a–d), comprising

[1]Department of Applied Geology, Curtin University of Technology, Kent Street, Bentley, Western Australia 6102, Australia. [2]The Research School of Earth Sciences, [3]Centre for Macroevolution and Macroecology, The Australian National University, Canberra, Australian Capital Territory 0200, Australia. [4]Centre for Microscopy, Characterisation and Analysis, The University of Western Australia, 35 Stirling Highway, Crawley, Western Australia 6009, Australia.

>50% kerogen (Fig. 1c, d). However, more commonly it is present as lenticular streaks surrounded by a mineral matrix (Fig. 1e). The kerogen resembles sedimentary organic matter termed 'lamalginite' in shales from the Palaeoproterozoic Barney Creek Formation, McArthur Group, northern Australia[20]. However, unlike the fluorescent kerogen in the mid-Proterozoic samples, which has yielded some of the oldest unambiguously syngenetic biomarkers[12,21], the Neoarchaean kerogen is opaque, non-fluorescent and highly reflective, indicative of higher thermal maturity.

The shales also contain irregular-to-circular masses of pyrobitumen dispersed in the mineral matrix (Fig. 2a–e) and, locally, lining the walls of crosscutting hydrothermal veins (Fig. 2f, g). The solid spheres and circular outlines, which are encased in pyrite (Fig. 2a–c), represent former oil droplets that have been converted to pyrobitumen during thermal alteration that caused significant volume loss (Fig. 2a–c). Residual oil is a common constituent of younger source rocks[20,22]. With increased burial and heating, oil is destroyed by means of cracking reactions, forming solid and insoluble pyrobitumen that becomes increasingly enriched in $^{13}C$ owing to the loss of isotopically depleted methane[22].

The preservation of solidified oil droplets and pore-filling pyrobitumen (Fig. 2a–e) deeply embedded within metamorphosed, organic-rich shale provides strong evidence for former *in situ* oil generation and primary migration. The intergrowth of pyrobitumen with authigenic pyrite that displays evidence of differential compaction suggests that oil may have formed before deep burial. The optical properties of the pyrobitumen, including high reflectivity and the absence of fluorescence, combined with ubiquitous shrinkage cracks (Fig. 2e), is typical of metamorphosed petroleum. These properties are shared with co-occurring kerogen ($R_{max} > 4.5\%$; $n = 3$), and are consistent with the metamorphic grade of the samples (200–300 °C)[18]. The severe thermal alteration experienced by the organic matter in these shales is incompatible with the preservation of indigenous hydrocarbon biomarkers.

Carbon isotopic measurements on individual kerogen and pyrobitumen particles were carried out to test whether oil generated in the Jeerinah shales is enriched in $^{13}C$ relative to the associated kerogen[4]. Because of the minute size of most of the organic residues, a NanoSIMS 50 ion microprobe was used to carry out *in situ* $^{13}C/^{12}C$ measurements at high spatial resolution (typically 5 μm by 5 μm; see Methods Summary and ref. 16 for detailed analytical procedures). All $\delta^{13}C$ values are reported relative to the Pee Dee Belemnite standard, and full data tables are available in Supplementary Information.

*In situ* analysis of kerogen in streaks and laminae (Fig. 1a–e) yielded $\delta^{13}C$ values ranging between –47.2‰ and –36.6‰ ($n = 20$; Fig. 3, see Supplementary Table 2), which is similar to the carbon isotopic composition of bulk organic matter[5,8] (Fig. 3). The $\delta^{13}C$ values for pyrobitumen in the shale matrix vary between –50.7‰ and –36‰ ($n = 69$; Fig. 3), and suggest that, on average, the indigenous oil is slightly more depleted in $^{13}C$ than co-occurring kerogen (Fig. 3; see Supplementary Table 2). The carbon isotopic results show that the soluble hydrocarbons are enriched in $^{13}C$ by 10–20‰ relative to matrix pyrobitumens and source kerogens (from which the biomarkers were reportedly extracted). On the basis of the carbon isotopic results and textural relationships, it is likely that the strongly $^{13}C$-depleted pyrobitumen was derived from co-occurring kerogen in

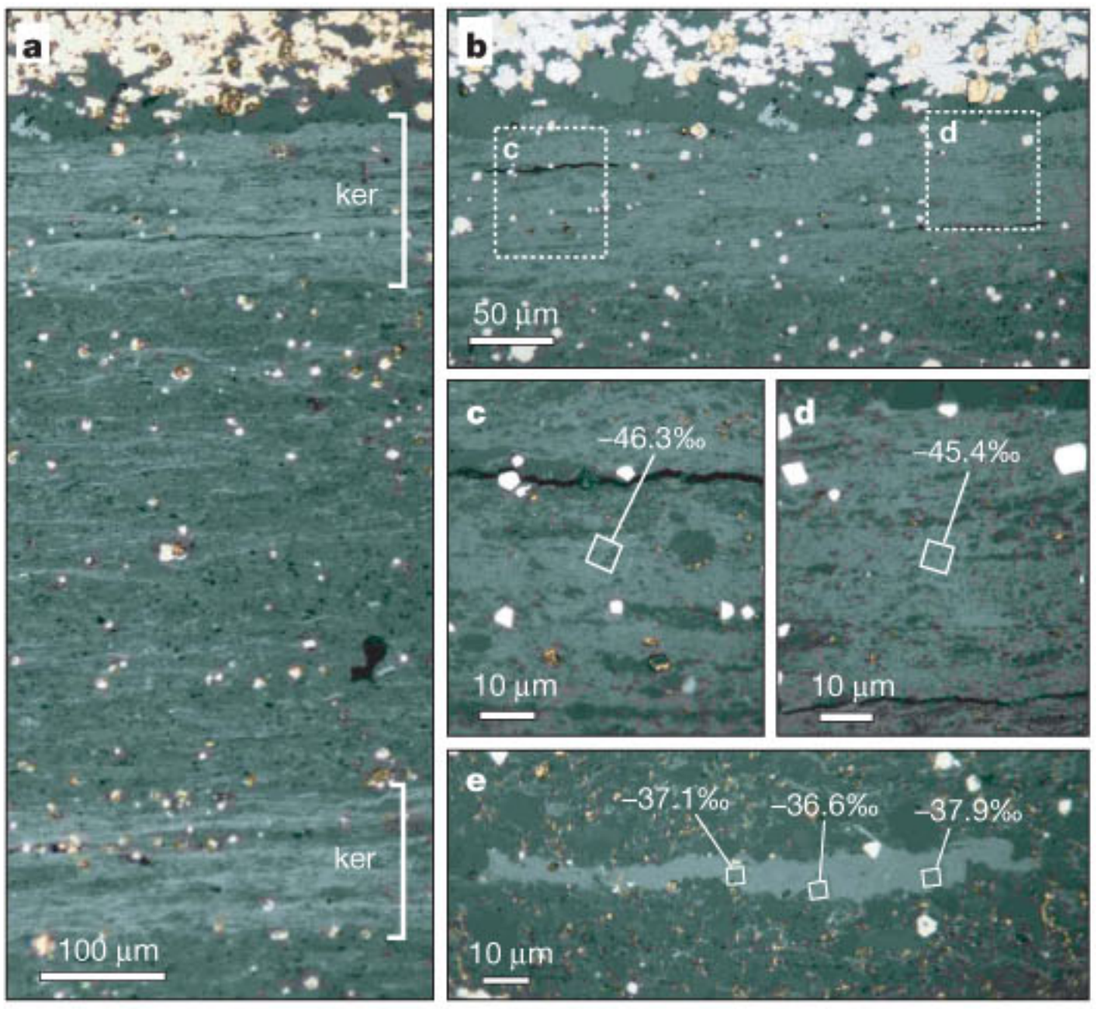


**Figure 1 | Reflected light photomicrographs of kerogen.** **a**, Two bands containing abundant kerogen laminae (ker). **b**, Close-up of the kerogen-rich layer (top) in **a**, located between pyrite-rich (white) and kerogen-poor (dark grey) matrix. **c**, **d**, Close-up of two areas in kerogen-rich band in **b** (two insets) showing areas of analysis (white box) and their $\delta^{13}C$ values. **e**, Isolated streak of kerogen with three analytical areas (white squares) and corresponding $\delta^{13}C$ values. $\delta^{13}C = 1000\{[(^{13}C/^{12}C)_{sample}/(^{13}C/^{12}C)_{standard}] - 1\}$.

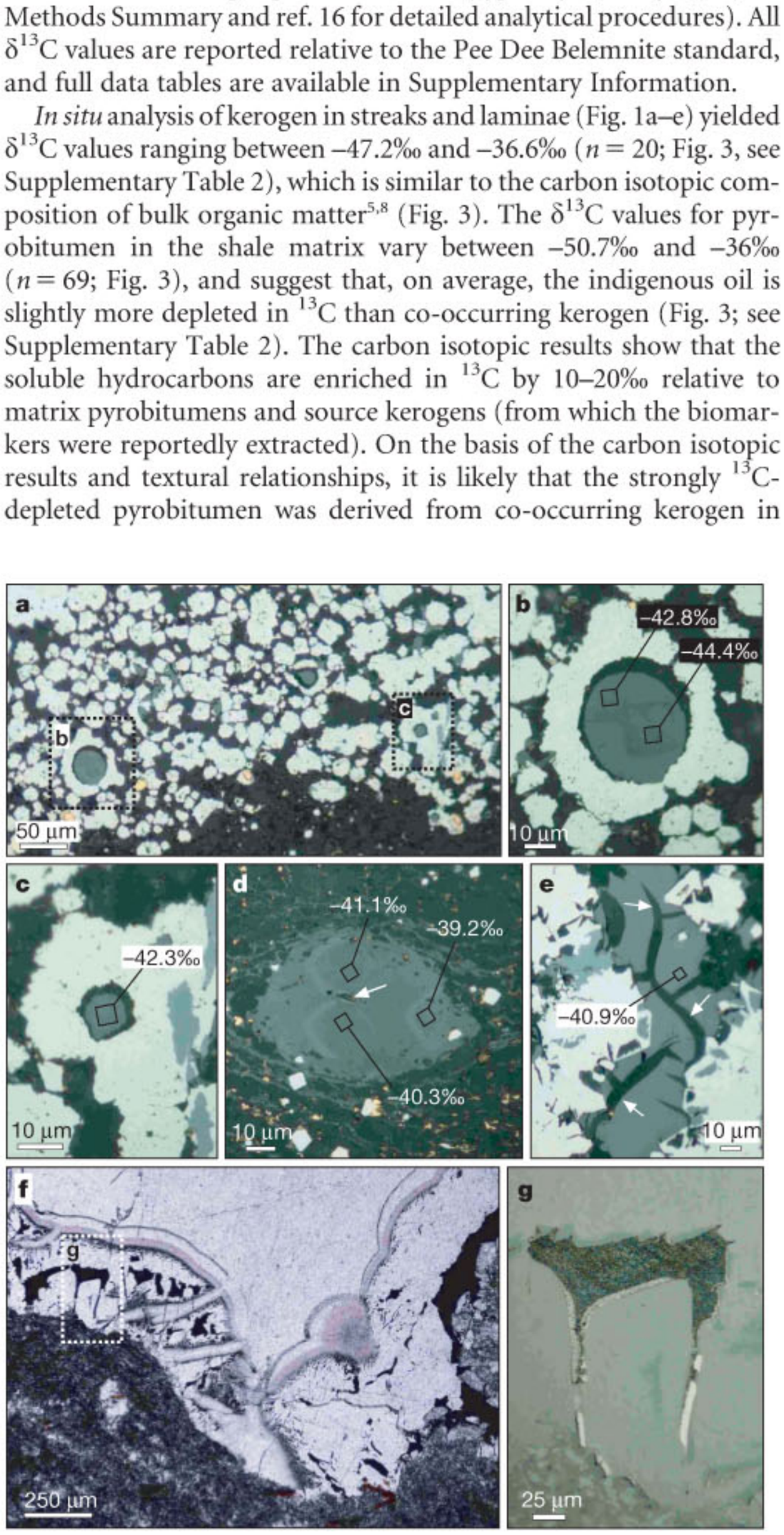


**Figure 2 | Reflected light photomicrographs (a–e, g) and a plane-polarized light photomicrograph (f) of pyrobitumen.** **a**, Band of authigenic pyrite (white) containing abundant pyrobitumen spheres and circular outlines (see insets). **b**, Close-up of solid pyrobitumen sphere (grey) surrounded by pyrite rim (white). Black squares represent analysis areas with corresponding $\delta^{13}C$ values. **c**, Minute pyrobitumen globule engulfed by pyrite (white) with a single analytical area and $\delta^{13}C$ value. The gap between the pyrobitumen and pyrite (in **b** and **c**) reflects shrinkage due to post-engulfment thermal cracking of former oil droplets. **d**, A nodule comprising a U-rich mineral core (see arrow) surrounded by pyrobitumen (grey). Three black outlines represent analytical areas with $\delta^{13}C$ values. Arrow, U-rich core. **e**, Irregular mass of pyrobitumen (grey) within authigenic pyrite (white). Sinuous shrinkage cracks (see arrows) indicate extensive thermal alteration of former oil. **f**, Opaque pyrobitumen (black) lining the margins of a hydrothermal vein. **g**, Close-up of pyrobitumen (inset in **f**) partly surrounding a vein-lining crystal that has been replaced by sparry carbonate.

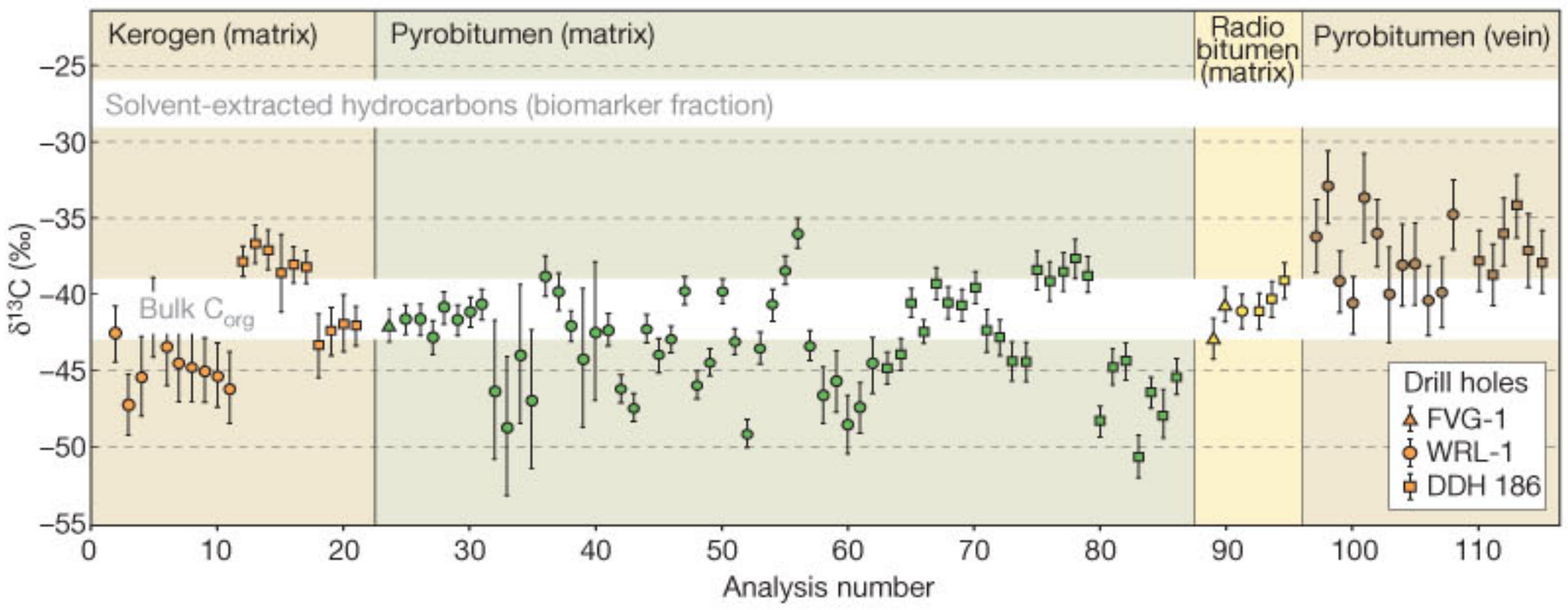


**Figure 3 | Carbon isotopic composition of organic matter.** The carbon isotopic fields for most of the solvent-extracted hydrocarbons[5] (white) and bulk organic matter[5,8] (white) from the Roy Hill Shale Member have been included for comparison. The precision of individual data points is indicated by vertical lines (1$\sigma$). The data points are listed in the order of appearance in Supplementary Table 2.

the Jeerinah shales. The production of highly $^{13}C$-depleted petroleum suggests that a methanotrophic biomass made a substantial contribution to the oil-producing lipids, supporting models for increased rates of methanogenesis in the Neoarchaean[13]. Owing to the absence of *n*-alkanes and isoprenoids derived from $^{13}C$-depleted membrane lipids of methanotrophs[4], it is difficult to explain how the molecular fossils could have been derived from organic matter indigenous to the ~2.63-Gyr-old shales. The extreme isotopic disparity between oil generated in the shale and hydrocarbons extracted from the shale is thus inconsistent with a syngenetic origin for the molecular fossils.

The pyrobitumen in younger veins in the shale (Fig. 2f, g) is $^{13}C$-enriched relative to matrix pyrobitumen and kerogen (Fig. 3), suggesting that oil migrated through the shales from an isotopically distinct, external source. This $^{13}C$-enriched pyrobitumen was not identified in the shale matrix, and, given its high thermal maturity, it also is unlikely to be the source of the *n*-alkanes and biomarkers extracted from the shales. Numerous episodes of post-Archaean fluid flow have been recognized in the region, ranging in age from 2.4 Gyr ago to <1.0 Gyr ago[9,23]. Each of these events may have transported non-indigenous organic molecules into the Neoarchaean shales. However, the liquid, non-pyrolytic bitumens must have entered the rocks after peak thermal alteration, which occurred over a 50-million-year (Myr) interval between 2.2 and 2.15 Gyr ago, on the basis of U–Pb dating of low-grade metamorphic monazite in the shales[9]. These dates also provide a maximum age for biomarkers extracted from the ~2.5-Gyr-old Mt McRae Shale[5,7], which was also heated to prehnite–pumpellyite facies by the same event[9].

Biomarkers have also been extracted from Archaean rocks of similar metamorphic grade in South Africa[24]; however, their origin and age remain uncertain[12]. Quartz-pebble conglomerates from the 2.45- to 2.21-Gyr-old Huronian Supergroup, Canada, contain oil-bearing fluid inclusions and yielded biomarkers for cyanobacteria and eukaryotes[25]. The inferred maximum age of the oil-bearing fluid inclusions is only constrained by the timing of peak metamorphism (upper prehnite–pumpellyite to lower greenschist facies; up to ~350 °C), which probably occurred during orogeny 1.89–1.8 Gyr ago. However, the low thermal maturity of the biomarkers and the presence of post-Devonian plant waxes[26] suggest a contribution from post-metamorphic molecular fossils. If the biomarkers detected in Archaean and early Palaeoproterozoic rocks are not indigenous, then a reassessment of the previously presented evidence for the first appearance of oxygenic photosynthesis, cyanobacteria[7] and eukaryotes[4] is required.

It has been proposed that oxygen-producing cyanobacteria evolved shortly before the Great Oxidation Event between 2.45 and 2.32 Gyr ago, triggering the collapse of a methane greenhouse and plunging the planet into a series of extreme glaciations[3]. However, the biomarker evidence for cyanobacteria and eukaryotes 2.7 Gyr ago[4–6] suggested a much earlier origin for oxygenic photosynthesis and a protracted interval (~300 Myr) of oxygenation, spawning several hypotheses for the long delay[27,28]. Our results suggest that the evidence provided by molecular fossils for the advent of oxygenic photosynthesis in the Archaean is not valid. Although cyanobacteria may have evolved during the Archaean, there is currently no evidence that requires it. Our findings also negate the use of cyanobacterial and eukaryotic biomarkers from 2.7- to 2.5-Gyr-old rocks as calibration points for molecular clocks and the universal tree of life.

There is possible geochemical evidence from late Archaean shales for trace amounts of oxygen ~2.5 Gyr ago[29]. However, the strongest indirect evidence for the appearance of oxygenic cyanobacteria is the rapid accumulation of atmospheric oxygen between 2.45 and 2.32 Gyr ago[1]. The oldest morphological fossils of clearly cyanobacterial affinity are only ~2.15 Gyr old[11], and the oldest fossils that are probably eukaryotic are 1.78–1.68 Gyr old[10]. If the origin of oxygenic photosynthesis postdated most of the Archaean, then this would strengthen arguments that phylogenetically older anoxygenic phototrophic bacteria that oxidize ferrous iron were responsible for the deposition of Archaean banded iron formations[30]. In addition, the production of extreme $^{13}C$-depleted organic matter in a pre-oxic environment would favour the presence of anaerobic[14] rather than aerobic[13] methanotrophic microbes. Our results eliminate the prime source of evidence for oxygenic photosynthesis before 2.5 Gyr ago[4–6] and the ~300 Myr delay in oxygen accumulation[27,28], rendering permissive models that link the emergence of cyanobacteria with an immediate rise of atmospheric oxygen and subsequent extreme glaciations[3].

## METHODS SUMMARY

Polished thin sections were prepared from drill core samples of the Roy Hill Shale Member (Fortescue Group) and examined by optical and scanning electron microscopes. Isotopic measurements were performed using the Cameca NanoSIMS 50 ion microprobe at the University of Western Australia. A ~1 pA $Cs^+$ primary ion beam was rastered across 5 × 5 μm areas of the sample surface. The $^{12}C^-$ and $^{13}C^-$ secondary ions were recorded simultaneously on electron multipliers. Carbon isotope ratios were determined from the total number of $^{12}C^-$ and $^{13}C^-$ counts recorded during each analysis, with corrections for electron-multiplier dead-time and the effects of quasi-simultaneous secondary ion arrivals (QSA). Measurements of kerogen and pyrobitumen in the sample were bracketed between measurements of the K-1 carbon standard under identical analytical conditions, and converted to $\delta^{13}C$ values normalized to the K-1 standard ($\delta^{13}C_{PDB} = -29.1‰$).

**Full Methods** and any associated references are available in the online version of the paper at www.nature.com/nature.

**Received 13 April; accepted 28 August 2008.**

1. Bekker, A. *et al.* Dating the rise of atmospheric oxygen. *Nature* **427**, 117–120 (2004).
2. Canfield, D. E. The early history of atmospheric oxygen. *Annu. Rev. Earth Planet. Sci.* **33**, 1–36 (2005).

3. Kopp, R. E., Kirschvink, J. L., Hilburn, I. A. & Nash, C. Z. The Paleoproterozoic snowball Earth: a climate disaster triggered by the evolution of oxygenic photosynthesis. *Proc. Natl Acad. Sci. USA* **102,** 11131–11136 (2005).
4. Brocks, J. J., Logan, G. A., Buick, R. & Summons, R. E. Archean molecular fossils and the early rise of eukaryotes. *Science* **285,** 1033–1036 (1999).
5. Brocks, J. J., Buick, R., Logan, G. A. & Summons, R. E. Composition and syngeneity of molecular fossils from the 2.78 to 2.45 billion-year-old Mount Bruce Supergroup, Pilbara Craton, Western Australia. *Geochim. Cosmochim. Acta* **67,** 4289–4319 (2003).
6. Brocks, J. J., Buick, R., Summons, R. E. & Logan, G. A. A reconstruction of Archean biological diversity based on molecular fossils from the 2.78 to 2.45 billion-year-old Mount Bruce Supergroup, Hamersley Basin, Western Australia. *Geochim. Cosmochim. Acta* **67,** 4321–4335 (2003).
7. Summons, R. E., Jahnke, L. L., Hope, J. M. & Logan, G. A. 2-Methylhopanoids as biomarkers for cyanobacterial oxygenic photosynthesis. *Nature* **400,** 554–557 (1999).
8. Hayes, J. M., Kaplan, I. R. & Wedeking, K. W. in *Earth's Earliest Biosphere: Its Origin and Evolution* (ed. Schopf, J. W.) 93–134 (Princeton Univ. Press, 1983).
9. Rasmussen, B., Fletcher, I. R. & Sheppard, S. Isotopic dating of the migration of a low-grade metamorphic front during orogenesis. *Geology* **33,** 773–776 (2005).
10. Knoll, A. H., Javaux, E. J., Hewitt, D. & Cohen, P. Eukaryotic organisms in Proterozoic oceans. *Phil. Trans. R. Soc. B* **361,** 1023–1038 (2006).
11. Hofmann, H. J. Precambrian microflora, Belcher Islands, Canada: Significance and systematics. *J. Paleontol.* **50,** 1040–1073 (1976).
12. Brocks, J. J., Grosjean, E. & Logan, G. A. Assessing biomarker syngeneity using branched alkanes with quaternary carbon (BAQCs) and other plastic contaminants. *Geochim. Cosmochim. Acta* **72,** 871–888 (2008).
13. Hayes, J. M. in *Early Life on Earth* (ed. Bengtson, S.) 220–236 (Columbia Univ. Press, 1994).
14. Hinrichs, K.-U. Microbial fixation of methane carbon at 2.7 Ga: was an anaerobic mechanism possible? *Geochem. Geophys. Geosyst.* **3,** 1–10 (2002).
15. Hoefs, J. *Stable Isotope Geochemistry* 158 (Springer, 2004).
16. Fletcher, I. R., Kilburn, M. R. & Rasmussen, B. NanoSIMS μm-scale in situ measurement of $^{13}C/^{12}C$ in early Precambrian organic matter, with permil precision. *Int. J. Mass Spec.* (in the press).
17. Rasmussen, B. Evidence for pervasive petroleum generation and migration in 3.2 and 2.63 billion-year old shales. *Geology* **33,** 497–500 (2005).
18. Smith, R. E., Perdrix, J. L. & Parks, T. C. Burial metamorphism in the Hamersley Basin, Western Australia. *J. Petrol.* **23,** 75–102 (1982).
19. Des Marais, D. J. in *Stable Isotope Geochemistry* (eds Valley, J. W. & Cole, D. R.) 555–578 (Reviews in Mineralogy and Geochemistry, Vol. 43, Mineralogical Society of America, 2001).
20. Crick, I. H., Boreham, C. J., Cook, A. C. & Powell, T. G. Petroleum geology and geochemistry of middle Proterozoic McArthur Basin, northern Australia II: assessment of source rock potential. *Am. Assoc. Petrol. Geol. Bull.* **72,** 1495–1514 (1988).
21. Summons, R. E., Powell, T. G. & Boreham, C. J. Petroleum geology and geochemistry of the middle Proterozoic McArthur Basin, northern Australia: III. Composition of extractable hydrocarbons. *Geochim. Cosmochim. Acta* **52,** 1747–1763 (1988).
22. Hunt, J. M. *Petroleum Geochemistry and Geology* (Freeman, 1995).
23. Rasmussen, B., Fletcher, I. R., Muhling, J. R., Thorne, W. S. & Broadbent, G. C. Prolonged history of episodic fluid flow in giant hematite ore bodies: Evidence from in situ U-Pb geochronology of hydrothermal xenotime. *Earth Planet. Sci. Lett.* **258,** 249–259 (2007).
24. Sherman, L. S., Waldbauer, J. R. & Summons, R. E. Improved methods for isolating and validating indigenous biomarkers in Precambrian rocks. *Org. Geochem.* **38,** 1987–2000 (2007).
25. Dutkiewicz, A., Volk, H., George, S. C., Ridley, J. & Buick, R. Biomarkers from Huronian oil-bearing fluid inclusions: An uncontaminated record of life before the Great Oxidation Event. *Geology* **34,** 437–440 (2007).
26. George, S. C., Volk, H., Dutkiewicz, A., Ridley, J. & Buick, R. Preservation of hydrocarbons and biomarkers in oil trapped inside fluid inclusions for >2 billion years. *Geochim. Cosmochim. Acta* **72,** 844–870 (2008).
27. Kump, L. R. & Barley, M. E. Increased subaerial volcanism and the rise of atmospheric oxygen 2.5 billion years ago. *Nature* **448,** 1033–1036 (2007).
28. Goldblatt, C., Lenton, T. M. & Watson, A. J. Bistability of atmospheric oxygen and the Great Oxidation. *Nature* **443,** 683–686 (2006).
29. Anbar, A. D. *et al.* A whiff of oxygen before the Great Oxidation Event? *Science* **317,** 1903–1906 (2007).
30. Konhauser, K. O. *et al.* Could bacteria have formed the Precambrian banded iron formations? *Geology* **30,** 1079–1082 (2002).


**Supplementary Information** is linked to the online version of the paper at www.nature.com/nature.

**Acknowledgements** We thank S. Bengtson, G. A. Logan, J. R. Muhling, S. Revets and S. Sheppard for discussion and comments; and A. C. Cook for organic reflectivity measurements. We acknowledge the facilities of the Australian Microscopy and Microanalysis Research Facility at the Centre for Microscopy, Characterisation and Analysis, University of Western Australia, a facility funded by the University, State and Commonwealth Governments.

**Author Information** Reprints and permissions information is available at www.nature.com/reprints. Correspondence and requests for materials should be addressed to B.R. (B.Rasmussen@curtin.edu.au).

## METHODS

**Samples and sample preparation.** Organic-rich shale from the Roy Hill Shale Member (Fortescue Group) was sampled from three drill cores—WRL-1 (22° 11.7′ S, 118° 12.6′ E), DDH 186 (22° 24′ S, 117° 55′ E) and FVG-1 (22° 33′ S, 119° 30′ E)—in the southern Pilbara Craton, Western Australia. Polished thin sections of the shale were prepared and examined by optical microscopy and scanning electron microscopy. Areas containing suitably large masses of organic matter were drilled out as 3-mm discs and set into 10-mm epoxy resin mounts with similar discs containing the K-1 standard. The mounts were coated with gold to provide electrical conductivity across non-conductive matrix minerals.

**Analytical procedures.** *In situ* isotopic measurements were performed using the Cameca NanoSIMS 50 ion microprobe at the University of Western Australia. Further information on the analytical procedures is given in ref. 16. All analyses were obtained by rastering a ~1 pA $Cs^+$ primary ion beam across 5 × 5 μm areas of the sample. The secondary ion species $^{12}C^-$, $^{13}C^-$, $^{16}O^-$ and $^{12}C^{14}N^-$ were recorded simultaneously by electron multipliers. The regions of interest were located using real-time secondary electron and $^{12}C^{14}N^-$ ion imaging. The instrument was tuned to achieve high mass resolution to separate the isobaric interference of $^{12}C^1H^-$ from $^{13}C^-$. For most analyses, a $^{12}C^-$ ion image acquired after the analysis was used to determine coverage (*p* of ref. 16) of the analyte in the rastered area. However, for analytical sessions 4 and 5, *p* was determined (with poorer precision) from subsequent $^{12}C^-$ images of a small selection of the original analysis areas, scanning electron microscope images and count rates. This is a major contributor to the overall uncertainties in some of the data from session 4. The $^{16}O^-$ signal was used to record supplementary images of the sample/matrix distribution. Taking images after analyses also allowed a check for local (that is, within the analysis raster area) sample charging. One analysis was rejected on this basis.

Interspersed analyses of the in-house K-1 carbon standard ($\delta^{13}C_{PDB} = -29.1$‰; ref. 16) were used to correct for drift in recorded ratios and to determine absolute $\delta^{13}C_{PDB}$ values. Data were collected in ten analytical sessions (Supplementary Table 1) over four months. Raw $^{13}C/^{12}C$ ratios were corrected for electron multiplier dead-time, and corrected for QSA by determining the primary-to-secondary ion ratio for each measurement and applying the first-order equation of ref. 31. Where necessary, the dead-time and QSA corrections were modified to account for incomplete coverage (ref. 16). Because there is some question concerning the general validity of the QSA model[32,33], we have re-calculated the data using the empirical QSA factors for carbon from ref. 33 (data not shown). This increases the final $\delta^{13}C_{PDB}$ values for low-count-rate analyses, but only several of the vein analyses with low count rates increase by >5‰. For the pyrobitumen and kerogen data, the average shift is <2‰ and there is no significant change in the data distributions.

All the data are plotted session-by-session in Supplementary Fig. 1, and are listed in Supplementary Table 2. The uncertainties shown for sample $\delta^{13}C$ include the 1$\sigma$ random statistical components from internal precision (the greater of Gaussian counting precision and block-to-block reproducibility), scatter around the K-1 standard regression in excess of the reproducibility expected from internal precision, and the estimated uncertainty in *p*. A notional systematic uncertainty in the QSA model (±10% of the QSA correction) has been added linearly to the statistical uncertainty. Uncertainties in the mean values and slopes of the K-1 regressions (generally <1‰ total) and the absolute value (0.24‰) have not been added.

31. Slodzian, G., Chaintreau, M., Dennebouy, R. & Rousse, G. Precise in situ measurements of isotopic abundances with pulse counting of sputtered ions. *Eur. Physical J. Appl. Physics* **14**, 199–232 (2001).
32. Slodzian, G., Hillion, F., Stadermann, F. J. & Zinner, E. QSA influences on isotopic ratio measurements. *Appl. Surf. Sci.* **231–232**, 874–877 (2004).
33. Hillion, F., Kilburn, M. R., Hoppe, P., Messenger, S. & Weber, P. K. The effect of QSA on S, C, O and Si isotopic ratio measurements. *Geochim. Cosmochim. Acta* **72**, A377 (2008).